Atmos. Chem. Phys. Discuss., 12, 12423–12451, 2012
www.atmos-chem-phys-discuss.net/12/12423/2012/
doi:10.5194/acpd-12-12423-2012

Atmospheric Chemistry and Physics Discussions

Implications of all season Arctic sea-ice anomalies on the stratosphere

D. Cai, M. Dameris, H. Garny, and T. Runde

Deutsches Zentrum für Luft- und Raumfahrt, Institut für Physik der Atmosphäre, Oberpfaffenhofen, Germany

Received: 13 February 2012 – Accepted: 2 May 2012 – Published: 15 May 2012

Correspondence to: D. Cai (duy.cai@dlr.de)

Published by Copernicus Publications on behalf of the European Geosciences Union.

Abstract

In this study the impact of a substantially reduced Arctic sea-ice cover on the lower and middle stratosphere is investigated. For this purpose two simulations with fixed boundary conditions (the so-called time-slice mode) were performed with a Chemistry-Climate Model. A reference time-slice with boundary conditions representing the year 2000 is compared to a second sensitivity simulation in which the boundary conditions are identical apart from the polar sea-ice cover, which is set to represent the years 2089–2099.

Three features of Arctic air temperature response have been identified which are worth to be discussed in detail. Firstly, tropospheric mean polar temperatures increase up to 7 K during winter. This warming is primarily driven by changes in outgoing long-wave radiation. Secondly, temperatures decrease significantly in the summer stratosphere caused by a decline in outgoing short-wave radiation, accompanied by a characteristic increase of ozone mixing ratios. Thirdly, there are short periods of statistical significant temperature anomalies in the winter stratosphere probably driven by modified planetary wave activity.

Both the internal as well as the inter-annual variability of Arctic sea-ice content is related to Arctic climatic fields like surface air temperature, sea level pressure or precipitation, which are analogue with the variability of the Arctic Oscillation (AO)-index. In this study significant changes in the AO-index are detected in the course of winter. Neutral phases of AO appear more often. As expected, the dominating dynamical response of the stratosphere during winter turned out to be consistent to alterations in the tropospheric AO, although it is not statistically significant most of the time.

1 Introduction

Arctic sea-ice cover has considerable declined in the current century and further decreases are predicted by general circulation models estimating an increase of

greenhouse gas concentrations (IPCC, 2007). Clear loss of Arctic sea-ice has been observed with the largest rate of decline in late summer months (e.g. Deser and Teng, 2008). Climate models predict a nearly ice-free summer in the Arctic within the coming 15–50 yr (e.g. Holland et al., 2006). But it must be taken into account that observed sea-ice reduction in recent years was much stronger than predicted by climate models, e.g. the IPCC AR4 models (Wu et al., 2006; Stroeve et al., 2007; Maslanik et al., 2007; Holland et al., 2007; see also Fig. 1 in Scinocca et al., 2009), offering the possibility of a quicker disappearance of Arctic sea-ice in summer and autumn.

Observational (e.g. Francis et al., 2009) as well as numerical modelling studies (see Budikova, 2009 for a comprehensive review) have suggested that sea-ice anomalies have a pronounced spatial and temperoral impact on the overlying atmosphere. Numerous investigations have been performed pointing out significant changes in tropospheric conditions (e.g. storm-track distribution and strength over mid- and high latitudes, air temperature, precipitation, etc.; Magnusdottir et al., 2004; Deser et al., 2004, 2010; Alexander et al., 2004; Singarayer et al., 2006; Seierstad and Bader, 2009).

It turned out that the leading empirical orthogonal function coefficients of sea-ice area can be related to Arctic Oscillation (AO), the dominating northern hemispheric variability pattern (Wang and Ikeda, 2000). This oscillation exhibits a negative phase with comparatively high pressure over the Arctic region and low pressure at midlatitudes (about 45° N), and a positive phase in which the pattern is reversed. Tropospheric weather patterns during a negative phase tend to damp the initialisation of planetary waves and contrary planetary wave activity is favoured during a positive phase. Trends in most of the Arctic climatic fields like surface air temperature, sea level pressure or precipitation is congruent with the variability of the AO (Thompson et al., 2000). Due to the relationship of northern hemispheric variability pattern and planetary waves there is a clear correlation of the AO-index and stratospheric conditions. During winter, this dominating tropospheric variability mode is intimately coupled to the variability of the strength of the stratospheric polar vortex (e.g. Thompson and Wallace, 1998; Wang and Ikeda, 2000; Black, 2002; Baldwin and Dunkerton, 2005; Scaife et al., 2005; Rind

et al., 2005): A positive AO-index corresponds to an anomalously strong polar vortex, while an anomalously weak polar vortex is found when the tropospheric circulation anomalies are of opposite sign.

Alterations in tropospheric conditions due to sea-ice retreat (e.g. changes in meridional temperature gradient or storm-track distribution and strength) could affect planetary wave forcing. Since stratospheric conditions strongly interact with planetary wave activity potential stratospheric feedback mechanism can be expected.

Scinocca et al. (2009) also raised the issue of stratospheric response to Arctic sea-ice reduction. Therefore they studied the sensitivity of Northern Hemisphere polar ozone recovery to complete sea-ice loss during summer. Based on long-term numerical simulations with the Canadian Middle Atmosphere Model (CMAM), i.e. a Chemistry-Climate Model (CCM) coupled to an ocean general circulation model, they found significant surface warming and stratospheric cooling in the North Polar region during March. Scinocca and colleagues showed that circulation changes in the troposphere are similar to those found in other studies (see above) and that they cause reduced planetary wave forcing of the stratosphere in response to the sea-ice loss. Consequently, downwelling over the North Polar region in March was reduced and therefore (dynamical) cooling over the polar region together with a reduced downward flux of ozone into the polar middle stratosphere was leading to less ozone. Unfortunately, Scinocca and coworkers did not provide additional information about stratospheric implications in other months.

This paper aims to identify and quantify impacts of a seasonally ice-free Arctic Ocean on stratospheric dynamics during all seasons and to investigate in more detail the cause and effect relationship of the stratospheric response to the prescribed sea-ice modifications. To our knowledge this is the first attempt to figure out the possible influence of a nearly sea-ice-free summer and fall season in the Arctic on stratospheric dynamics over the whole year. The paper is organised in the following way: the next section provides a brief repetition of the most important features of the CCM E39CA which is used for this study and a comprehensive description of the model

set-up chosen for the numerical simulations. In Sect. 3 the results of analyses are presented and discussed. At first the Arctic tropospheric and stratospheric response are shown. Stratospheric results are separated in winter and summer response. Then tropospheric-stratospheric interaction is analysed with the help of meridional eddy heat flux and AO-index. In the final section a summary and some conclusions are given.

2 Model description and set-up of simulations

2.1 Model description

We are analysing two simulations performed with the CCM E39CA. The spectral horizontal resolution is T30, which correspond roughly to 3.75° × 3.75° on the transformed latitude-longitude grid. The vertical partitioning of the model extent from surface to 10 hPa occurs in 39 layers using sigma-pressure coordinates. E39CA is based on spectral general circulation model ECHAM4.L39(DLR) (Land et al., 1999) with substantially improving model performance upgrades such as the chemistry-module CHEM (Steil et al., 1998) and the fully Lagrangian advection scheme ATTILA (Reithmeier and Sausen, 2002). More details of E39CA can be found in Stenke et al. (2008) and Stenke et al. (2009). The present used model version E39CA was part in the extensive intermodel comparison and evaluation project CCMVal-2 (SPARC CCMVal et al., 2010). It has been pointed out an overall good model performance in the upper troposphere and lower stratosphere (Gettelman et al., 2010; Hegglin et al., 2010), which is an advantage when investigating tropospheric-stratospheric interactions.

2.2 Simulation set-ups

To identify the atmospheric response of Arctic sea-ice content (ASIC) two simulations were conducted in the so-called timeslice mode, i.e. the equilibrium climate state of one period is simulated by varying only the intra-annual and keeping the inter-annual

boundary conditions constant. Each simulation was integrated over a 20-yr timing cycle following a 5 yr spin-up.

The reference simulation (REF) describes the climate mean state of the last decade. Boundary conditions were reinforced at values representative for the year 2000. Concentrations for long-lived greenhouse gases are based on IPCC (2001) and concentrations of ozone depleting substances follows values of WMO (2007). The lower boundary conditions stem from HadGEM1 (Martin et al., 2006; Johns et al., 2006). SSTs and sea-ice cover are the climatological 10-yr mean of the seasonal cycle over 1995–2004 of the HadGEM SSTs. Further reading for REF set-up see Garny et al. (2011).

Apart from the lower boundary conditions the "perturbed" simulation run (NO-ICE) is identical to REF. Compared to REF the SSTs of NO-ICE are invariant but sea-ice cover is replaced by the climatological mean of the seasonal cycle over 2089–2098 of the HadGEM SSTs. Due to the extreme reduction of sea-ice cover gaps arises at the edges between "future" ice surface areas and "extra-arctic" SST fields. These gaps were filled by interpolation of SST values of the present and the future.

Figure 1 shows the prescribed ASIC in terms of seasonal means. In REF maximum in the extend of ASIC is during DJF and MAM. Sea-ice covers the whole Arctic Ocean and big parts of its surrounding oceans. In the course of summer the ice surface reduces continuously and reaches its minimum in autumn, but sea-ice is still left in the area of the North Polar sea. The situation in NO-ICE is fundamentally different. In contrast to REF most of the surrounding Arctic waters are ice-free, like Bering Strait or sea of Okhotsk in the North-east Pacific. Especially in summer, ASIC is almost completely removed.

3 Results

The following investigations are based on comparisons between the two E39CA timeslice simulations REF and NO-ICE which differ from each other only in the prescribed Arctic sea-ice distributions. In summer and autumn months ASIC is the most different

(Fig. 1). The analyses presented here focus on the all season stratospheric response to the predefined lower boundary conditions in all seasons.

Meridional seasonal means of stratospheric fields like temperature, zonal wind and ozone concentration derived from REF and NO-ICE yield statistically significant differences mainly in high northern latitudes (not shown). Therefore, the subsequent analyses concentrate on middle to high latitudes of the Northern Hemisphere. Figure 2 shows climatological mean temperature differences for the North Polar region (60°–90° N) as derived from the two simulations (i.e. NO-ICE minus REF). The climatological means are based on 20-yr of daily model data in each case (see Sect. 2). There are three features of interest which will be discussed in the following: (A) The Arctic tropospheric temperature changes, (B) the Arctic stratospheric temperature response in summer, and (C) the Arctic stratospheric temperature response in winter and early spring.

3.1 Arctic tropospheric response (area A)

Before the stratospheric response is discussed in detail (subsequent subsections), the strength and the seasonal behaviour of tropospheric temperature changes in the Arctic are compared to respective values mentioned in some of the previous studies presented in Sect. 1. This allows a quantification of the direct tropospheric temperature response in E39CA to the applied sea-ice perturbation in comparison to other similar investigations (see Sect. 2.2).

In contrast to the anomalies of Arctic sea-ice content (NO-ICE minus REF) (Fig. 1), the temperature response is greatest in early winter (November, December). Temperature increase in the NO-ICE simulation is found roughly from August to April with a maximum temperature increase at ground level of up to 7 K in late November. Only a slight warming near the surface is detected from May to July. This diametric behaviour of temperature and ASIC is contributed to the ocean-atmosphere temperature gradient; during winter months ASIC recovers but the surface heat flux (latent and sensible) from the open waters to the overlying cold atmosphere is enhanced and leads

to an anomalous warming of the lower Arctic atmosphere (e.g. Parkinson et al., 2001; Singarayer et al., 2006; Serreze et al., 2009; Kumar et al., 2010; Overland and Wang, 2010). Generally, the surface air temperature (SAT) anomaly pattern mostly reflects the prescribed design of sea-ice reduction; locally, SAT differences in December can reach 20 K (not shown). The detected temporal evolution as well as the strength of SAT anomalies is in agreement with results presented in other studies (e.g. Singarayer et al., 2006). The temperature signal is limited to lower model layers. In accordance with Deser et al. (2004), statistically significant anomalies are mostly identified in the boundary layer. The maximum vertical extent is found in mid December when a robust temperature signal is found up to about 4 km.

In response to the seasonal ocean-atmosphere temperature gradient changes the differences in outgoing long-wave (LW) radiative flux at the surface is largest in periods of greatest temperature anomalies (Fig. 6b). Beginning in August and lasting to February there is a marked increase of LW upward radiative flux. In the course of early winter the difference between NO-ICE and REF reaches a maximum of 31 $W m^{-2}$ whereas during summer differences are only in the order of 2.5 to 3 $W m^{-2}$. Consistent to Alexander et al. (2004) maximum values of LW outgoing radiation response can locally exceed 100 $W m^{-2}$ (not shown). Moreover, water vapour concentrations in the boundary layer (not shown) are significantly enhanced during periods of significant temperature rising.

3.2 Arctic summer stratospheric response (area B)

In the stratosphere above about 23 km a statistically significant cooling of approx. 0.5 K is identified from the beginning of July to the end of August (Fig. 2). This cooling is likely related to changes in short-wave (SW) radiation (Fig. 6a) which are most obvious from May to August. As prescribed, during summer the greatest changes in Arctic sea-ice content occur and hence changes in surface albedo are most obvious at that time. A great extent of highly reflecting sea-ice is replaced by comparable dark open water. The maximum descent of SW reflecting radiation of 21 $W m^{-2}$ near the surface

of the North Polar region is found in July. During late spring and summer the stratosphere in NO-ICE is generally colder than in REF which is consequent to the reduction of reflected SW radiation. The statistical insignificance of the negative stratospheric temperature response in late spring/early summer and early fall (which has the same order of magnitude) is caused by enhanced inter-annual variability in these seasons.

Obviously higher stratospheric ozone mixing ratios up to 40 ppb are detected in NO-ICE between June and August (Fig. 3). Although the change of ozone mixing ratio is relatively small (i.e. about 1 %) it is statistically significant since the internal variability during summer is very low. In principle the positive ozone signal is contemporaneous to the negative one of stratospheric temperature. This connection is explained by well understood temperature dependencies of ozone destroying chemical reactions at altitudes above around 25 km; the catalytic reactions of ozone depletion can significantly slow down by lower temperatures (e.g. Haigh and Pyle, 1982; Dameris, 2010; Chapt. 4 in WMO, 2011).

3.3 Arctic extented-winter (November–March) stratospheric response (area C)

Figure 2 offers a very prominent and statistically significant cooling of the stratosphere in the NO-ICE simulation arising in the second half of November (significance level 95 %) and continuous with smaller values until mid December. The maximum difference between REF and NO-ICE is −4.5 K. Statistical significance in November is even robust for the 99 % level. During this time ozone anomalies (Fig. 3) are only statistically significant in the lower stratosphere below roughly 22 km. From January to mid of April the stratospheric domain is most of the time dominated by positive temperature anomalies, but there are shorter episodes of cooling in late February and in the middle of March. In total the stratospheric temperature response from the beginning of the year to early spring ranges from −1.5 K to 1.5 K. The mid winter and early spring months (December–March) response in the North Polar region is only significant for the 75 % level due to the high internal variability (not shown). Nevertheless, in the following

we explore in more detail potential connections of changes in Northern atmospheric circulation patterns and corresponding dynamical feedbacks to the stratosphere.

3.4 Meridional heat fluxes

The zonal mean of the meridional eddy heat flux ($\overline{v'T'}$) in middle latitudes can be used as a measure of atmospheric wave activity.

The annual development of the mean meridional heat flux response (NO-ICE minus REF) is shown in Fig. 4, while only the stationary component is given in Fig. 5. It turned out that the transient component is mainly insignificant all the year round and therefore it is not shown. In the stratosphere alterations of meridional heat flux can roughly be found during extended winter period (November–March). In November significant weakening in NO-ICE of total $\overline{v'T'}$ can be recognised. Particularly the stationary component offers a very clear decline. Total values decrease by about 18 $\mathrm{K\,m\,s^{-1}}$ which is roughly 24 % of the climatological mean value. In the remaining time the response is mainly insignificant.

In general the stationary component of the meridional heat flux dominates the anomaly pattern of total $\overline{v'T'}$. From January on, the influence of transient component of $\overline{v'T'}$ anomaly is getting stronger, associated with enhanced variability which contributes to less statistical differences.

However obvious analogies in the structure can be recognised comparing the anomaly pattern of Arctic temperature and middle latitude eddy heat flux. According to Newman et al. (2001) during winter terms there is a linear correlation of $\overline{v'T'}$ of mid latitudes in the lower stratosphere (100 hPa) and Arctic temperature of the middle stratosphere (30 hPa) when dynamical processes in the atmosphere are comparatively strong indicating a dynamical feedback of polar vortex temperatures and planetary wave activity.

In particular during November a very clear response in temperature and meridional heat flux can be identified. It also must be mentioned that ASIC reaches its smallest

expansion during November to February and hence potential heat release from open waters is comparatively high. November is the only month where a statistically significant and consistent geopotential anomaly can be found through every level of the atmosphere. The tropospheric low pressure system located at the Aleutian islands (Fig. 7) is significantly weakened. Looking at stratospheric levels (Fig. 8) the wave number 1 pattern dominates the geopotential response pattern. In this case this is associated with a shift of polar vortex centre from Asia to the middle of the Arctic carrying out a dynamical stabilisation of the polar vortex. Consistent to this both the stationary component of $\overline{v'T'}$ and stratospheric temperatures decrease. Corresponding interactions of Aleutian low and polar vortex are also shown in context of modification of northern hemispheric leading atmospheric circulation pattern (e.g. Overland et al., 1999; Ambaum et al., 2001).

3.5 Leading pattern of Northern Hemisphere AO

As already mentioned in the introduction the stratosphere is intimately connected to the leading variability pattern of atmospheric circulation. Strong positive index values and large changes in ice conditions in the late 1980s through early 1990s contributed to the conclusion that the AO was the most dominant atmospheric circulation regime affecting Arctic climate (Thompson and Wallace, 1998).

For this study daily AO-indices are constructed by projecting the daily mean 1000-hPa height anomalies polewards of 20° N onto the leading EOF (Empirical Orthogonal Function) mode (for more details regarding this issues see Hurrell and Deser, 2009).

From November to March frequency distribution of AO-indices offers in the NO-ICE simulation a growing number of near-neutral phase and at the same time a tendency of decreasing comparatively high and low AO-index values (Fig. 9). Alterations tested with a chi-square test are significant at a 99 % level. This is analogue to recent studies which determined for the last decade a shift from strongly positive AO-index values to more neutral AO-indices during winter while sea-ice gradually is reduced (e.g. Overland and Wang, 2005; Maslanik et al., 2007; Zhang et al., 2008). Generally the coupling of

stratospheric conditions and AO is seen most clearly when comparing the strongest with the weakest anomalies (e.g. Baldwin and Dunkerton, 2005). Due to an increasing number of near-neutral AO events in NO-ICE an enhanced stratospheric variability during extended winter period is not expected. In consistency to this, stratospheric temperature and eddy heat fluxes show mainly insignificant responses during winter months with the exception of November. Analysis of monthly frequency distribution of AO-index reveals for November prominent differences to the distribution (Fig. 10). AO values are shifted on average to higher values corresponding to a more stable polar vortex. For the remaining months frequency distribution is either insignificant following a chi-square test or AO amplitudes alter randomly (not shown).

Often AO is associated with Arctic climate change. As already mentioned in the introduction trends of Arctic surface climate indicators like SAT or sea-ice cover are congruent with the variability of the AO. But in the last decade AO-indices tend to be more neutral in difference to the almost linear trends of Arctic climatic fields.

Hence suggestions appeared that the Arctic has passed a tipping point into a new climatic state and AO has less influence on Arctic climate (e.g. Lindsay and Zhang, 2005; Maslanik et al., 2007; Zhang et al., 2008). On the other hand Arctic stratospheric temperature, serving as an indicator for the strength of the polar vortex, also shows this episodic character (Overland and Wang, 2005). However our results show consistencies in alterations of AO-indices and stratospheric response. In particular during November AO-indices clearly shift to more positive values which corresponds to a stronger polar vortex at this time.

4 Summary and conclusions

In this study, the atmospheric response to prescribed sea-ice anomalies was investigated. The detected tropospheric responses, for example temporal evolution and strength of SAT anomalies (locally exceeding 20 K), offer consistent results to previous

comparable studies (e.g. Deser et al., 2004; Alexander et al., 2004; Singarayer et al., 2006).

Further analyses expanded to the stratosphere mainly yield statistically relevant differences in middle to high northern latitudes.

Generally the stratospheric response is small compared to the inter-annual variability. Hence statistically significant changes are detected during summer when stratospheric dynamical variability is weak. In the course of the summer months significant stratospheric temperature response decreases about −0.5 K. Upwelling SW radiation is strongly reduced due to major changes in sea-ice cover and thus surface albedo. This consequently contributes to stratospheric cooling in this period. Contemporaneously ozone mixing ratio increases about 1 %. This coupling is explained by temperature dependencies of ozone destroying chemical reactions in the middle stratosphere.

From November to March planetary wave activity analysed with values of the meridional eddy heat flux ($\overline{v'T'}$) indicates consistent results to stratospheric Arctic temperature response. Both temperature and $\overline{v'T'}$ anomalies yielding mainly insignificant results apart from November. Stationary waves dominate the dynamical winter response while from January on enhanced alterations in the transient component of $\overline{v'T'}$ contribute to a higher inter-annual variability and less statistical significance. In our simulation setup sea-ice anomalies yielding the most prominent response during November. Atmospheric alterations result in a stronger polar vortex associated with stable stratospheric conditions (i.e. lower temperatures). Former studies highlighted the influence of initial state of polar vortex on the whole winter period.

Solely in November significant geopotential height anomalies can be detected continuously from troposphere to stratosphere. In stratospheric layers geopotential anomalies depict a shift of polar vortex from Eurasia to the Arctic carrying out a dynamical stabilisation.

Analogue to recent studies the AO-index in NO-ICE is shifted to near neutral-phase. However our results show consistencies in alterations of AO indices and stratospheric response. In particular during November AO-indices clearly shift to more positive

values which corresponds to a stronger polar vortex. But generally during November to March AO reflects a rather indistinct stratospheric response which is also depicted in analyses of temperature and meridional eddy heat flux concerning statistical significance.

The response shown here of the lower and middle stratosphere to sea-ice loss is comparatively small over the whole year. The strong tropospheric temperature forcing during winter has no statistically detectable influence on the stratosphere due to a high variability driven by planetary wave activity. In the summer months tropospheric temperature response is relatively weak but significant stratospheric changes arises from radiational effects due to major changes in the surface albedo.

Configurations of our sensitivity study is an attempt to display the atmospheric reaction on a hypothetical future sea-ice cover reduction in a climate representing the present state. Further efforts are required to gain general conclusions. So melting sea-ice could have a great impact on ocean circulation which affects atmospheric circulation pattern and vice versa (e.g. Aagaard and Carmack, 1989; Qiu and Jin, 1997). Predictions of future stratospheric scenarios should necessarily consider this potential oceanic feedback for reliable results.

Acknowledgements. This study was funded by the Deutsche Forschungsgemeinschaft (DFG) through the DFG-research group SHARP (stratospheric change and its role for climate prediction) under grant DA 233/3-1. We also want to thank Andreas Dörnbrack for helpful comments on the manuscript.

References

Aagaard, K. and Carmack, E. C.: The role of sea ice and other fresh water in the Arctic circulation, J. Geophys. Res., 94, 14485–14498, doi:10.1029/JC094iC10p14485, 1989. 12436

Alexander, M., Bhatt, U., Walsh, J., Timlin, M., Miller, J., and Scott, J.: The atmospheric response to realistic Artic sea ice anomalies in an AGCM during winter, J. Climate, 17, 890–905, 2004. 12425, 12430, 12435

Ambaum, M. H. P., Hoskins, B. J., and Stephenson, D. B.: Arctic oscillation or North Atlantic oscillation?, J. Climate, 14, 3495–3507, 2001. 12433
Baldwin, M. and Dunkerton, T.: The solar cycle and stratosphere-troposphere dynamical coupling, J. Atmos. Sol.-Terr. Phy., 67, 71–82, doi:10.1016/j.jastp.2004.07.018, 2005. 12425, 12434
Black, R. X.: Stratospheric forcing of surface climate in the Arctic Oscillation., J. Climate, 15, 268–277, 2002. 12425
Budikova, D.: Role of Arctic sea ice in global atmospheric circulation: a review, Global Planet. Change, 68, 149–163, 2009. 12425
Dameris, M.: Climate change and atmospheric chemistry: How will the stratospheric ozone layer develop?, Angew. Chem. Int. Edit., 49, 8092–8102, doi:10.1002/anie.201001643, 2010. 12431
Deser, C. and Teng, H.: Recent trends in Arctic sea ice and the evolving role of atmospheric circulation forcing, 1979–2007. in: Arctic Sea Ice Decline: Observations, Projections, Mechanisms, and Implications, Geophysical Monograph, 180, edited by: DeWeaver, E. T., Bitz, C. M., and Tremblay, L. B.,AGU, 7–26, 2008. 12425
Deser, C., Magnusdottir, G., Saravanan, R., and Phillips, A.: The effects of North Atlantic SST and sea ice anomalies on the winter circulation in CCM3. Part II: Direct and indirect components of the response, J. Climate, 17, 877–889, 2004. 12425, 12430, 12435
Deser, C., Thomas, R., Alexander, M., and Lawerence, D.: The seasonal atmospheric response to projected Arctic Sea ice loss in the late twenty-first-century, J. Climate, 23, 333–3351, 2010. 12425
Francis, J. A., Chan, W., Leathers, D. L., Miller, J. R., and Veron, D. E.: Winter Northern Hemisphere weather patterns remember summer Arctic sea-ice extent, Geophys. Res. Lett., 36, L07503, doi:10.1029/2009GL037274, 2009. 12425
Garny, H., Dameris, M., Randel, W., Bodeker, G. E., and Deckert, R.: Dynamically forced increase of tropical upwelling in the lower stratosphere, J. Atmos. Sci., 68, 1214–1233, doi:10.1175/2011JAS3701.1, 2011. 12428
Gettelman, A., Hegglin, M. I., Son, S.-W., Kim, J., Fujiwara, M., Birner, T., Kremser, S., Rex, M., Anel, J. A., Akiyoshi, H., Austin, J., Bekki, S., Braesike, P., Brühl, C., Butchart, N., Chipperfield, M., Dameris, M., Dhomse, S., Garny, H., Hardiman, S. C., Jöckel, P., Kinnison, D. E., Lamarque, J. F., Mancini, E., Marchand, M., Michou, M., Morgenstern, O., Pawson, S., Pitari, G., Plummer, D., Pyle, J. A., Rozanov, E., Scinocca, J., Shepherd, T. G., Shibata, K.,

Smale, D., Teyssdre, H., and Tian, W.: Multimodel assessment of the upper troposphere and lower stratosphere: tropics and global trends, J. Geophys. Res., 115D, D00M08, doi:10.1029/2009JD013638, 2010. 12427
Haigh, J. D. and Pyle, J. A.: Ozone perturbation experiments in a two-dimensional circulation model, Q. J. Roy. Meteor. Soc., 108, 551–574, 1982. 12431
Hegglin, M. I., Gettelman, A., Hoor, P., Krichevsky, R., Manney, L., G., Pan, L. L., Son, S.-W., Stiller, G., Tilmes, S., Walker, K. A., Eyring, V., and T. G. Shepherd, S., Waugh, D., Akiyoshi, H., Anel, J. A., Austin, J., Baumgaertner, A., Bekki, S., Braesicke, P., Brühl, C., Butchart, N., Chipperfield, M., Dameris, M., Dhomse, S., Frith, S., Garny, H., Hardiman, S. C., Jöckel, P., Kinnison, E. D., Lamarque, J. F., Mancini, E., Michou, M., Morgenstern, O., Nakamura, T., Olivi, D., Pawson, S., Pitari, G., Plummer, D. A., Pyle, J. A., Rozanov, E., Scinocca, J. F., Shibata, K., Smale, D., Teyssdre, H., Tian, W., and Yamashita, Y.: Multimodel assessment of the upper troposphere and lower stratosphere: extratropics, J. Geophys. Res., 115D, D00M09, doi:10.1029/2010JD013884, 2010. 12427
Holland, M. M., Bitz, C. M., and Tremblay, B.: Future abrupt reductions in the summer Artic sea ice, Geophys. Res. Lett., 33, L23503, 5pp., 2006, doi:10.1029/2006GL028024. 12425
Holland, M. M., Bitz, C. M., Tremblay, B., and Bailey, D. A.: The role of natural versus forced change in future rapid summer Arctic ice loss, in: Arctic Sea Ice Decline: Observations, Projections, Mechanisms, and Implications, Geophysical Monograph, 180, edited by: DeWeaver, E. T., Bitz, C. M., and Tremblay, L. B., AGU, 133–150, 2008. 12425
Hurrell, J. W. and Deser, C.: North Atlantic climate variability: the role of the North Atlantic oscillation, J. Marine Syst., 78, 28–41, doi:10.1016/j.jmarsys.2008.11.026., 2009. 12433
IPCC: Climate Change 2001 – The physical science basis, Tech. rep., Intergovernmental Panel on Climate Change, Cambridge University Press, New York, USA, 2001. 12428
IPCC: Climate Change 2007 – The physical science basis, Tech. rep., Intergovernmental Panel on Climate Change, Cambridge University Press, New York, USA, 2007. 12425
Johns, T. C., Durman, C. F., Banks, H. T., Roberts, M. J., McLaren, A. J., Ridley, J. K., Senior, C. A., Williams, K. D., Jones, A., Rickard, G. J., Cusack, S., Ingram, W. J., Crucifix, M., Sexton, D. M. H., Joshi, M. M., Dong, B., Spencer, H., Hill, R. S. R., Gregory, J. M., Keen, A. B., Pardaens, A. K., Lowe, J. A., Bodas-Salcedo, A., Stark, S., and Searl, Y.: The new Hadley Centre Climate Model (HadGEM1): evaluation of coupled simulations, J. Climate, 19, 1327–1353, 2006. 12428

Kumar, A., Perlwitz, J., Eischeid, J., Quan, X., Xu, T., Zhang, T., Hoerling, M., Jha, B., and Wang, W.: Contribution of sea ice loss to Arctic amplification, Geophys. Res. Lett., 37, L21701, doi:10.1029/2010GL045022, 2010. 12430

Land, C., Ponater, M., Sausen, R., and Roeckner, E.: The ECHAM4.L39 (DLR) Atmosphere GCM. Technical Description and Model Climatology, DLR Forschungsbericht 1999-31, 1999. 12427

Lindsay, R. W. and Zhang, J.: The thinning of Arctic sea ice, 1988–2003: have we reached a tipping point?, J. Climate, 18, 4879–4984, 2005. 12434

Magnusdottir, G., Deser, C., and Sarvanan, R.: The effects of North Atlantic SST and sea ice anomalies on the winter circulation in CCM3. Part I: Main features and storm track characteristics of the response, J. Climate, 17, 857–876, 2004. 12425

Martin, G. M., Ringer, M. A., Pope, V. D., Jones, A., Dearden, C., and Hinton, T. J.: The physical properties of the atmosphere in the new Hadley Centre Global Environmental Model (HadGEM1). Part 1: Model description and global climatology, J. Climate, 19, 1274–1301, 2006. 12428

Maslanik, J., Drobot, S., Fowler, C., Emery, W., and Barry, R.: On the Arctic climate paradox and the continuing role of atmospheric circulation in affecting sea ice conditions., Geophys. Res. Lett., 34, L03711, doi:10.1029/2006GL028269, 2007. 12425, 12433, 12434

Newman, P., Nash, E., and Rosenfield, J.: What controls the temperature of the Artic stratosphere during spring?, J. Geophys. Res., 106, 19999–20010, 2001. 12432

Overland, J. E. and Wang, M.: Arctic climate paradox: the recent decrease of the Arctic oscillation, Geophys. Res. Lett., 32, L06701, doi:10.1029/2004GL021752, 2005. 12433, 12434

Overland, J. E. and Wang, M.: Large-scale atmospheric circulation changes are associated with the recent loss of Arctic sea ice, Tellus A, 62, 1–9, doi:10.1111/j.1600-0870.2009.00421.x, 2010. 12430

Overland, J. E., Adams, J. M., and Bond, N. A.: Decadal variability of the Aleutian low and its relation to high-latitude circulation, J. Climate, 12, 1542–1548, 1999. 12433

Parkinson, C., Rind, D., Healy, R., and Martinson, D.: The impact of sea ice concentration accuracies on climate model simulations with the GISS GCM, J. Climate, 14, 2606–2623, 2001. 12430

Qiu, B. and Jin, F. F.: Antarctic circumpolar waves: an indication of ocean-atmosphere coupling in the extratropics, Geophys. Res. Lett., 20, 2585–2588, doi:10.1029/JC094iC10p14485, 1997. 12436

Reithmeier, C. and Sausen, R.: ATTILA: Atmospheric tracer transport in a Lagrangian model, Tellus B, 54, 278–299, 2002. 12427

Rind, D., Perlwitz, J., and Lonergan, P.: AO/NAO response to climate change: 1. Respective influences of stratospheric and tropospheric climate changes, J. Geophys. Res., 110, D12107, doi:10.1029/2004JD005103, 2005. 12425

Scaife, A. A., Knight, J. R., Vallis, G. K., and Folland, C. K.: A stratospheric influence on the winter NAO and North Atlantic surface climate, Geophys. Res. Lett., 32, L18715, 0.1029/2005GL023226, 2005. 12425

Scinocca, J. F., Reader, M., Plummer, P., Sigmond, M., Kushner, P., Shepherd, T., and Ravishankara, A.: Impact of sudden Artic sea-ice loss on stratospheric polar ozon recovery, Geophys. Res. Lett., 36, L24701, 5pp., doi: 10.1029/2009GL041239, 2009. 12425, 12426

Seierstad, I. and Bader, J.: Impact of a projected future Artic sea ice reduction on extratropical storminess and the NAO, Clim. Dynam., 33, 937–943, 2009. 12425

Serreze, M. C., Barrett, A. P., Stroeve, J. C., Kidig, D. N., and Holland, M. M.: The emergence of surface-based Arctic amplification, Cryosphere, 3, 11–19, 2009. 12430

Singarayer, J., Bamber, J., and Valdes, P.: Twenty-first-century climate impacts from a declining Arctic sea ice cover, J. Climate, 19, 1109–1125, 2006. 12425, 12430, 12435

SPARC CCM Val, Eyring, V., Shepherd, T., and Waugh, D. E.: SPARC CCMVal Report on the Evaluation of Chemistry-Climate Models, Tech. rep., SPARC Report No. 5, WCRP-132, WMO/TD-No. 1526, 2010. 12427

Steil, B., Dameris, M., Brühl, C., Crutzen, P. J., Grewe, V., Ponater, M., and Sausen, R.: Development of a chemistry module for GCMs: first results of a multiannual integration, Ann. Geophys., 16, 205–228, doi:10.1007/s00585-998-0205-8, 1998. 12427

Stenke, A., Grewe, V., and Ponater, M.: Lagrangian transport of water vapor and cloud water in the ECHAM4 GCM and its impact on the cold bias, Clim. Dynam., 31, 491–506, 2008. 12427

Stenke, A., Dameris, M., Grewe, V., and Garny, H.: Implications of Lagrangian transport for simulations with a coupled chemistry-climate model, Atmos. Chem. Phys., 9, 5489–5504, doi:10.5194/acp-9-5489-2009, 2009. 12427

Stroeve, J., Holland, M., Meier, W., Scambos, T., and Serreze, M.: Artic sea ice decline: faster than forecast, Geophys. Res. Lett., 34, L09501, 5pp., doi:10.1029/2007GL029703, 2007. 12425

Thompson, D. W. J. and Wallace, J. M.: The Arctic oscillation signature in the wintertime geopotential height and temperature fields, Geophys. Res. Lett., 25, 1297–1300, 1998. 12425, 12433

Thompson, D. W. J., Wallace, J. M., and Hegerl, G. C.: Annular modes in the extratropical circulation. Part II: Trends, J. Climate, 13, 1018–1036, 2000. 12425

Wang, J. and Ikeda, M.: Arctic oscillation and Arctic sea-ice oscillation, Geophys. Res. Lett., 27, 1287–1290, 2000. 12425

WMO: Scientific Assessment of Ozone Depletion: 2006, Tech. rep., WMO Global Ozone Research and Monitoring Project Report No. 50, Geneva, Switzerland, 2007. 12428

Wu, B., Wang, J., and Walsh, J. E.: Dipole anomaly in the winter Arctic atmosphere and its association with sea ice motion, J. Climate, 19, 210–225, 2006. 12425

Zhang, X., Sorteberg, A., Zhang, J., Gerdes, R., and Comiso, J. C.: Recent radical shifts of atmospheric circulations and rapid changes in Arctic climate system, Geophys. Res. Lett., 35, L22701, doi:10.1029/2008GL035607, 2008. 12433, 12434

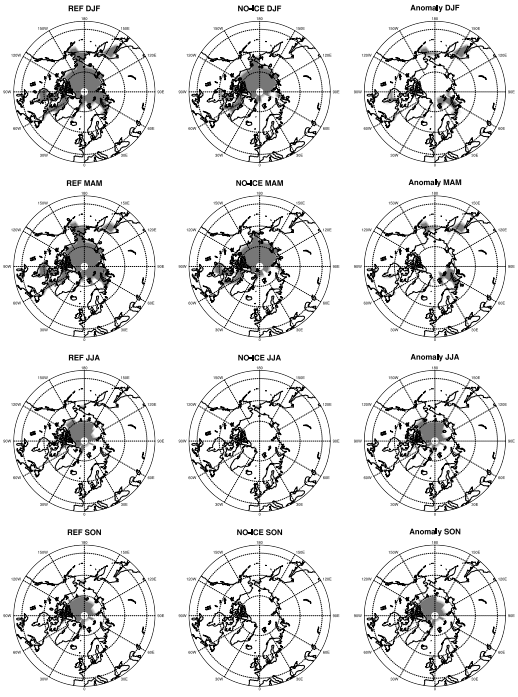

Fig. 1. First column: seasonal means of prescribed ASIC of REF; second column: seasonal means of prescribed ASIC of NO-ICE (grey illustrates areas covered by sea-ice); third column: anomaly = NO-ICE – REF (grey illustrates areas of reduced sea-ice).

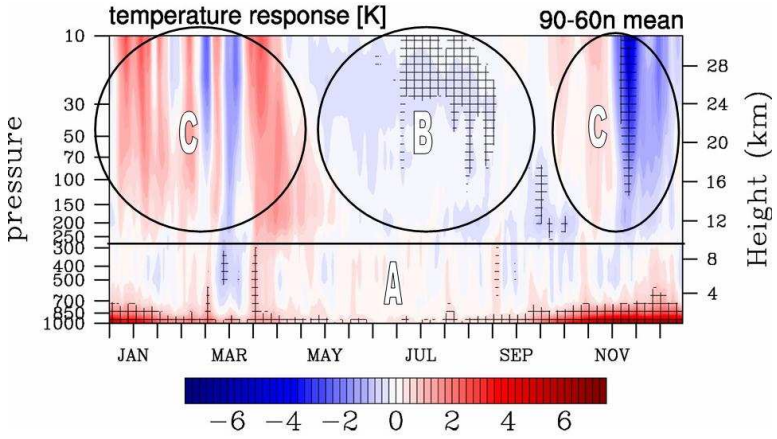

Fig. 2. Daily Arctic temperature response (NO-ICE – REF). Following student *t*-test shaded areas are significant at a 95 % level. Labeled ticks mark mid of the month.

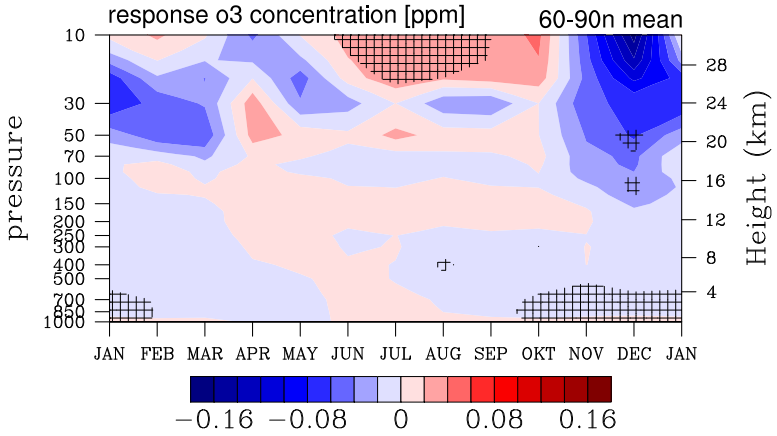

Fig. 3. Monthly mean Arctic ozone mixing ratio response (NO-ICE – REF). Following student *t*-test shaded areas are significant at a 95 % level.

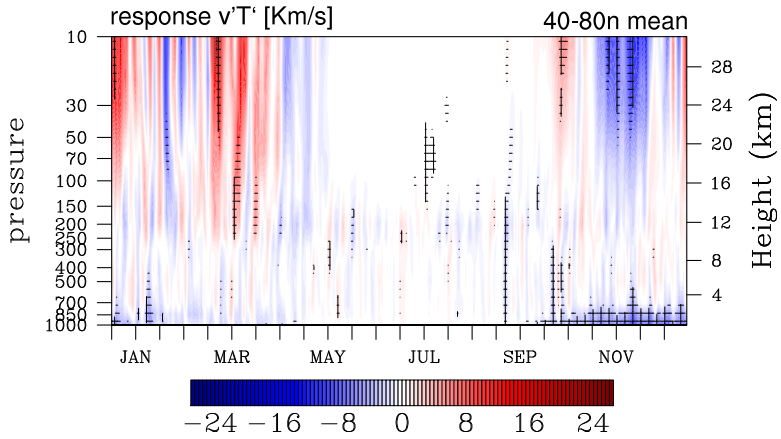

Fig. 4. Daily $\overline{v'T'}$ response (NO-ICE – REF) averaged from 40°–80° N. Following student t-test shaded areas are significant at a 95 % level. Labeled ticks mark mid of the month.

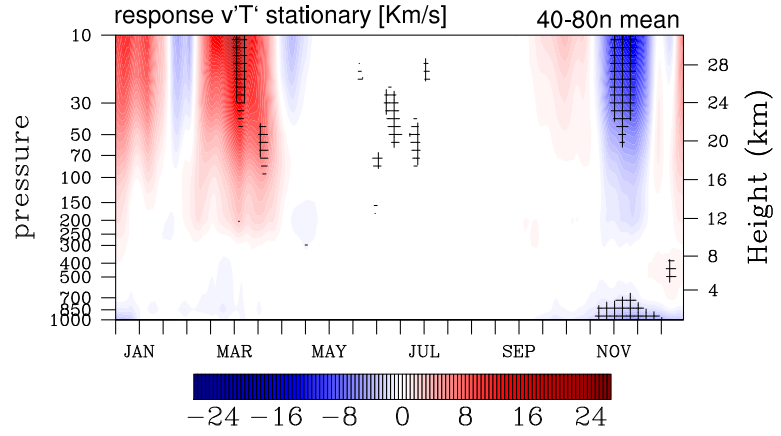

Fig. 5. Stationary component of daily $\overline{v'T'}$ response (NO-ICE – REF) averaged from 40°–80° N. Following student t-test shaded areas are significant at a 95 % level. Labeled ticks mark mid of the month.

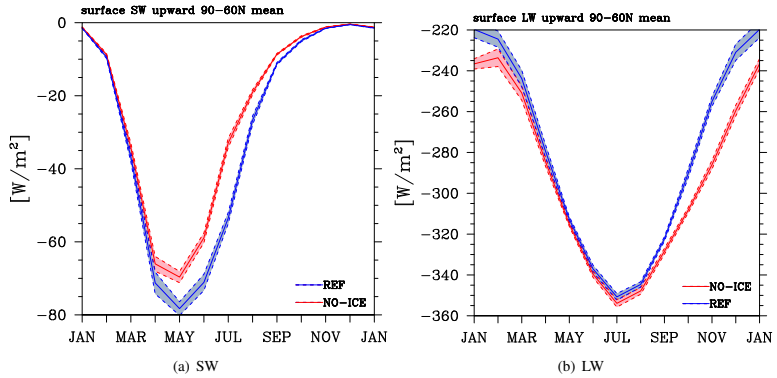

Fig. 6. Outgoing radiation from surface. **(a)** respective short-wave (SW) radiation averaged over Arctic region; **(b)** respective long-wave (LW) radiation averaged over Arctic region. Coloured area covers the 1σ-standard deviation.

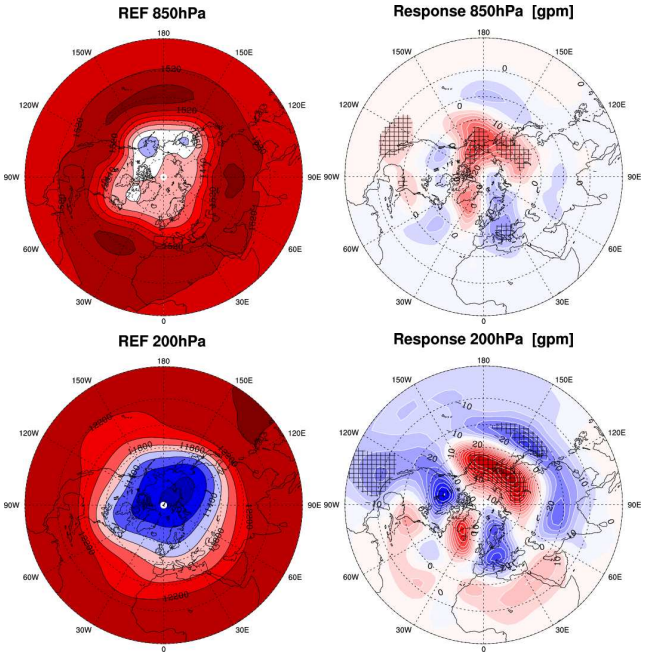

Fig. 7. Polar stereographic projections of REF simulation tropospheric geopotential at 850 hPa and 200 hPa (left column) in November, and respective response NO-ICE minus REF (right column). Shaded areas are significant at a 95 % level following student *t*-test.

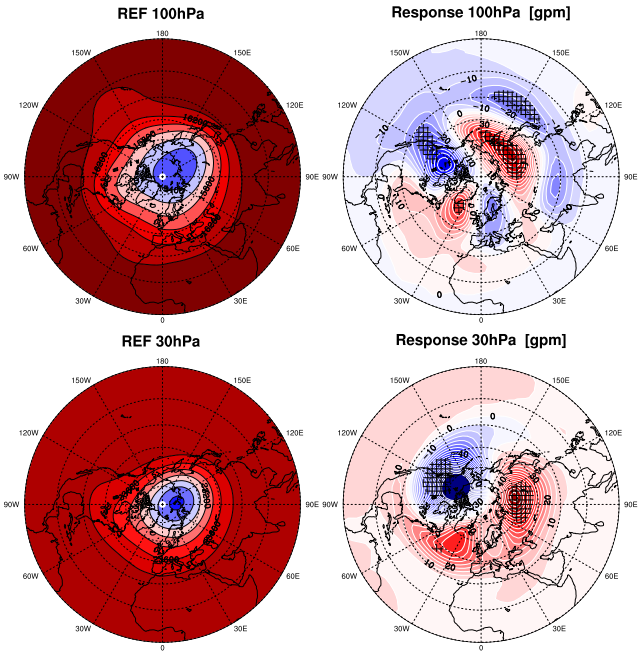

Fig. 8. Polar stereographic projections of REF simulation stratospheric geopotential at 100 hPa and 30 hPa (left column) in November, and respective response NO-ICE minus REF (right column). Shaded areas are significant at a 95 % level following student *t*-test.

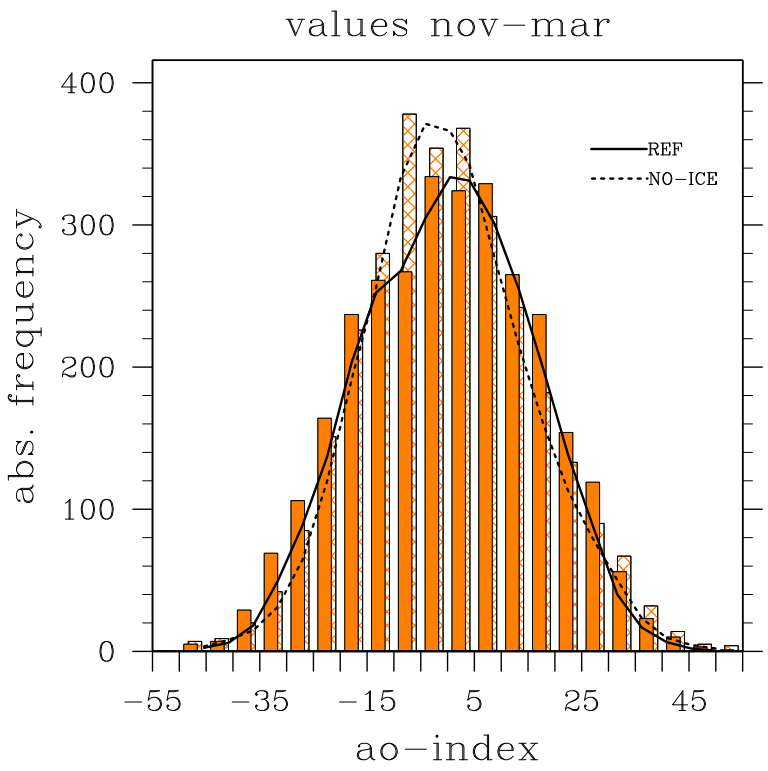

Fig. 9. Frequency distribution of AO indices for November–March. Solid and shaded lines are the running average of two adjacent bins.

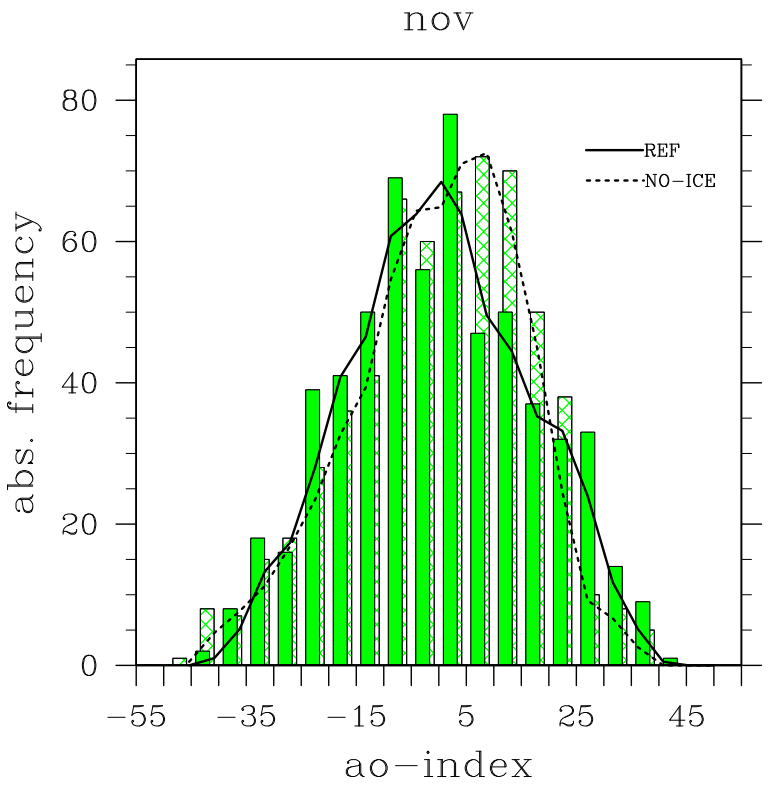

Fig. 10. Frequency distribution of November AO indices. Solid and shaded lines are the running average of two adjacent bins.